Utilization of the Paragominas mining tailings to obtain FAU zeolite: Synthesis optimization using a factorial DOE and Response Surface Methodology

Caio C. A. Melo [1], Bruna L. S. Melo[2], Rômulo S. Angélica[3] and Simone P. A. Paz[4]
1. R&D Specialist, Hydro, Belém, Brazil
2. Undergraduate Student
3, 4. Professor Researchers
University Federal of Pará, Belém, Brazil
Corresponding author: caio.melo@hydro.com

Abstract

The bauxite processed in the Mineração Paragominas SA has its content of reactive silica reduced by disaggregation/washing and classification stages. This process generates a significant amount of fine fraction rich in kaolinite, which is currently discarded in tailings dams. Considering the environmental liability regarding this disposal, this work investigates the technical feasibility for using the tailings waste material to produce zeolite – a material that has several industrial applications due to its microstructural characteristics. A sequential methodology of factorial design of experiments (DOE) and response surface methodology (RSM) was used to evaluate experimental variables that influence the production of synthetic FAU-type zeolite. The experiments were carried out in hydrothermal system using NaOH solution and the products were analyzed by XRD where peak intensities of the zeolitic phases were used as the response variables. A crystalline FAU zeolite was successfully produced. Among all the variables considered in this study the alkaline concentration, SiO_2 / Al_2O_3 molar ratio and time of reaction showed to be the most important factors for the FAU synthesis. In conclusion, the tailings proved to be a feasible resource to produce zeolitic materials and most influential parameters for this process were determined. The transformation of kaolinite rich tailings into a useful product could represent benefits in economic and environmental terms. Further studies should be done to evaluate the product's performance and potential market demands.

Keywords: Bauxite tailings, DOE, FAU-type Zeolite.

1. Introduction

The mining industry plays an important role in the Brazilian economy, and the Amazon region is a major center of mining of bauxite. According to the Mineral Summary 2016, the state of Pará - Northern Brazil - was responsible for 93.1 % of the national production of bauxite [1]. Despite its importance, the production bauxite generates a significant amount of tailings during ore processing. Currently, the tailings represent an environmental liability to the mining industry, especially in the Amazon region, where areas are deforested for their disposal, and because of its very fine particle size (< 4 μm), it hampers vegetation recovery [2, 3].

Most recently a quite similar clay material – kaolin tailings – have been widely studied on zeolite synthesis using it as cheap and environmentally friendly raw material. The results showed that it is technically feasible to produce several types of zeolites, such as NaA, NaP, Faujasite (FAU), chabazite and basic sodalite [4, 5, 6, 7, 8, 9]. Previous studies shown that the tailings generated by bauxite washing process (Mineração Paragominas - Norsk Hydro) is mainly composed of gibbsite (chemically represented as $Al_2O_3 \cdot 3H_2O$) and kaolinite ($Al_2O_3 \cdot 2SiO_2 \cdot 2H_2O$). This fact brings a glimpse to explore both kaolinite and gibbsite present in this waste as a source of SiO_2 and Al_2O_3 to produce zeolites. The concept to use of industrial tailings as raw material for the production of new materials with potential economic application can represent a sustainable approach with

financial and environmental returns for the industries and society, in this case, inserted in the Amazon region.

Several variables, such as metakaolinization [10], the SiO_2 / Al_2O_3 molar ratio [11, 12], the reaction medium alkalinity [13], temperature and time of synthesis, have been reported to be influencing factors for the zeolitization process, both in relation to the type of zeolite to be formed and its microstructural characteristics [14, 15, 16]. However, it is difficult to estimate what experimental conditions are adequate to synthesize only a specific phase for the following reasons: a) The number of possibly significant controllable variables in the reaction system is very large; in addition to the factors mentioned above (which are examined in this study), several others have been reported, such as the kaolin calcination conditions [17, 18, 19], aging conditions [20, 21, 22], and the presence of impurity minerals [23]; b) The factors are usually studied separately and at different levels, which makes it impossible to correlate reported results or to identify interactions between the factors [24]; and c) Some data cannot be reproduced under similar conditions, which makes it difficult to confirm the conclusions of other authors [23, 25].

For this reason, the present study aimed to investigate the best synthesis conditions for producing not only a zeolitic material (composed by several zeolite phases) but a FAU-type zeolite as the only synthesized material. Therefore, the factorial design of experiments (DOE) and response surface methodology (RSM) with the desirability tool were applied to determine an optimized experimental region and a regression model of FAU-type zeolite synthesis considering the most influential experimental factors. Such study appears to be a novel approach, both for transforming this tailings into something of economic value and for bringing together a large number of factors in the hydrothermal syntheses of FAU-type zeolites and analyzing their influence and interactions, which could be helpful for futures studies on FAU-type zeolite synthesis from clay minerals.

2. Experimental

All the experiments performed to obtain the zeolitic material were conducted in a hydrothermal system using Teflon lined stainless steel reactors (50 mL capacity), under autogenous pressure. It was used a fixed mass of the gibbsite-kaolinite waste (3 g) and volume of the NaOH solution (25 mL) varying the concentration of the alkaline solution. An amount of amorphous silica was added to ensure the SiO_2 / Al_2O_3 molar ratios desired – previously calculated from the content of SiO_2 and Al_2O_3 in the tailings. The reactors were placed in an oven for heating with the temperature and time varying. All the variable values were set according to the experimental design. After the syntheses, the products were filtered and washed using distilled water until pH ~7, dried in an oven at 105 °C for 6 hours, and analyzed by X-ray diffraction (XRD).

2.1. Materials

The raw materials used were the bauxite tailings (BT) from Mineração Paragominas SA - Norsk Hydro generated by ore washing/grading; an amorphous silica (commercially named SILMIX®) co-product from the silicon metal production by Dow Corning Metals of Pará. It is noteworthy that this amorphous silica was previously considered as an industrial mineral waste, however, due to its potential applications (mainly for the cement industry) it has become a co-product. Alkaline solution (NaOH) was used as the leaching agent and source of Na_2O for the zeolite.

2.2. Experimental Design

This whole study was based on a sequential experimental design methodology. In the first step, a fractional factorial design was conducted to determine the most significant variables. In the second step, after establishing the values of the less significant variables, a path of steepest ascent

was defined to an optimized experimental region. Finally, a composite factorial design was carried out in this new region to determine the optimized levels of the variables and the regression model using the RSM.

All the experiments were randomized and followed by the examination of residuals (complying with the assumptions of independence, randomness, homoscedasticity and normality) and an ANOVA test with a 95 % confidence interval. The response variables were the intensity values of the main XRD peaks of the Faujasite (FAU d_{111}) and basic sodalite (SOD d_{110}) phases identified in the products.

2.2.1. Fractional Factorial Design (2_V^{5-1})

The five-factor two-level factorial design with resolution *V* results in 16 experimental runs. However, 3 additional runs were added at the center point in order to perform a lack-of-fit test for curvature, totaling 19 runs. The design matrix is shown in Table 1. In these screening experiments were evaluated, therefore, five variables reported by many authors as important in the hydrothermal synthesis of zeolites: alkaline concentration, SiO_2 / Al_2O_3 molar ratio, temperature, time of reaction and heat treatment of the raw material (calcination). The descriptions of these variables and their original values are shown in Table 2.

Table 1. (2_V^{5-1}) fractional factorial design with coded variables.

Standard order	Coded Variables				
	X_1	X_2	X_3	X_4	X_5
1	-1	-1	-1	-1	+1
2	+1	-1	-1	-1	-1
3	-1	+1	-1	-1	-1
4	+1	+1	-1	-1	+1
5	-1	-1	+1	-1	-1
6	+1	-1	+1	-1	+1
7	-1	+1	+1	-1	+1
8	+1	+1	+1	-1	-1
9	-1	-1	-1	+1	-1
10	+1	-1	-1	+1	+1
11	-1	+1	-1	+1	+1
12	+1	+1	-1	+1	-1
13	-1	-1	+1	+1	+1
14	+1	-1	+1	+1	-1
15	-1	+1	+1	+1	-1
16	+1	+1	+1	+1	+1
17	0	0	0	0	0
18	0	0	0	0	0
19	0	0	0	0	0

Table 2. Factors and levels for the 2_V^{5-1} fractional factorial design.

Coded Variables	Original Variables	Levels		
		-1	**0**	**1**
X_1	Alkaline concentration (g/L)	200	260	320
X_2	SiO_2 / Al_2O_3 ratio	1.20	1.44	1.69
X_3	Temperature (ºC)	70	90	110
X_4	Time (h)	24	48	72
X_5	Calcination*	yes	-	no

** Calcination was performed at 700 ºC for 2h.*

2.2.2. Steepest Ascent

The experimental conditions adopted for the path of steepest ascent are described in Table 3. The origin, basic step size (ΔX) and slope of the path direction for each variable were determined from the first-order model using the response surfaces obtained from the desirability function, which was adjusted for FAU(d_{111})max and SOD (d_{110})min.

Table 3. Steepest ascent design.

Steps	Coded Variables			Original Variables		
	X_1	X_2	X_4	Alkaline concentration (g/L)	SiO_2 / Al_2O_3 ratio	Time (h)
Origin (0)	*0*	*0*	*0*	*260*	*1.45*	*48*
Δx	*-1*	*0.35*	*0.25*	*-20*	*0.09*	*6*
0+Δ1	1	0.35	0.25	240	1.54	54
0+Δ2	2	0.7	0.5	220	1.62	60
0+Δ3	3	1.05	0.75	200	1.71	66
0+Δ4	4	1.4	1.0	180	1.80	72
0+Δ5	5	1.75	1.25	160	1.88	78
0+Δ6	6	2.1	1.5	140	1.97	84
0+Δ7	7	2.45	1.75	120	2.06	90
0+Δ8	8	2.8	2.0	100	2.14	96

2.2.3. Central Composite Design (23)

Since it was possible to establish fixed values for some variables, as well as to find an experimental condition in the vicinity of the optimized region, it is possible to perform a full factorial design. Thus, the optimized FAU zeolite synthesis parameters from the cheap natural raw material (BT) can be known [26]. Tables 4 and 5 show the experimental matrix and the descriptions of the variables with their original values, respectively.

Table 4. 2^3 central composite design with coded variables.

Standard order	Coded Variables		
	X_1	X_2	X_3
1	-1	-1	-1
2	+1	-1	-1
3	-1	+1	-1
4	+1	+1	-1
5	-1	-1	+1
6	+1	-1	+1
7	-1	+1	+1
8	+1	+1	+1
9	-1.68	0	0
10	+1.68	0	0
11	0	-1.68	0
12	0	+1.68	0
13	0	0	-1.68
14	0	0	+1.68
15	0	0	0
16	0	0	0

Table 5. Factors and levels for the 2^3 central composite design.

Coded Variables	Original Variables	Levels				
		-1.68	**-1**	**0**	**+1**	**+1.68**
X_1	Alkaline concentration (g/L)	106.4	120	140	160	173.6
X_2	SiO_2 / Al_2O_3 ratio	1.82	1.88	1.97	2.06	2.12
X_4	Time (h)	74	78	84	90	94

2.3. Characterization

X-ray diffraction analysis was performed with a PANalytical Empyrean diffractometer with Co anode X-ray ceramic tubes ($K\alpha_1$ = 1.789010 Å), a long fine focus, a Kβ Fe filter, and a PIXcel3D-Medpix3 1x1 detector in scanning mode with a 40 kV voltage, a 35 mA current, a step size of 0.0065° 2θ, scanning from 2.0000° to 74.9980° 2θ, a time step of 30.600 s, the divergence slit set to 1/8°, the anti-scatter slit set to 1/4°, and a 10 mm mask.

The specific surface area, the pore volume and distribution size were obtained from N_2 adsorption measurements at 77 K using QUANTACHROME / Nova - 1200 analyzer. By these measurements the adsorption - desorption isotherms were obtained, using the BET method (Brunauer - Emmett - Teller) to estimate the specific surface area and calculating the pore distribution size and volume by the BJH method (Barrett - Joyner - Halenda). Before the adsorption measurements, the samples were pre-treated at 200 ºC for 4 h for degassing.

A morphological analysis was performed using a scanning electron microscope (SEM) Zeiss model SIGMA-VP with EDS IXRF model Sedona-SD coupled. The operating conditions were: electron beam current = 80 μA, constant acceleration voltage = 20 kV, working distance = 11.9 mm.

3. Results and Discussion

3.1. Characterization of the Raw Materials

The diffractograms of the raw materials are shown in Figure 1. The phases identified in the BT sample are gibbsite, kaolinite, hematite, Al-goethite and anatase. The mineralogical quantification of this material was estimated by Nascimento et al. [6], who showed that the major phase is ~48.0 % gibbsite, followed by ~32.0 % kaolinite, and all the other phases, including amorphous phases, represent approximately 20.0 % wt. This information supports the expectation that this material is a good source of Al_2O_3 and SiO_2 to produce zeolites. The diffraction pattern of BT calcined at 700 °C shows that both kaolinite and gibbsite were fully amorphized since no reflections of these phases were found. As expected, the diffractogram of the SILMIX® is also characteristic of an amorphous material.

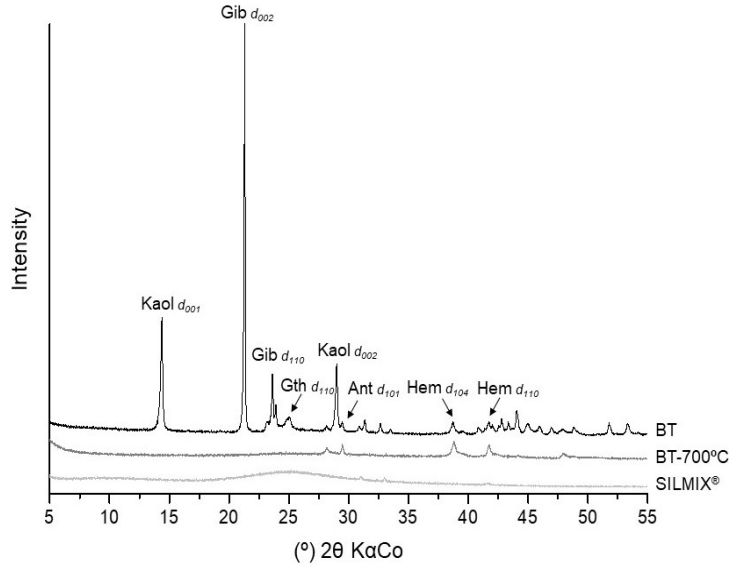

Figure 1. XRD pattern of the raw materials. Legends: Kaol: kaolinite; Gib: gibbsite; Gth: goethite; Ant: anatase; Hem: hematite.

3.2. Main Experimental Factors

To determine the experimental factors that most influence the synthesis of FAU-type zeolite with good crystallinity, a fractional factorial design with resolution V (2_V^{5-1}) was performed. This experimental design is very useful for performing screening experiments, mainly when many factors must be analyzed, and the appropriate experimental region is not well known [27, 28].
Figure 2 shows the diffractograms of several products obtained. The zeolite phases EMT, FAU, NaA, NaP and basic sodalite were observed under the conditions tested; these phases were also obtained in similar experiments that started with kaolin and metakaolin [4, 5, 7, 8, 12, 15]. However, the predominant phases in this experimental region were basic sodalite and FAU zeolite, respectively.

The delay in zeolitization caused by the addition of amorphous silica reported by Lapides & Heller-Kallai [24] was not observed, and good FAU zeolite formation was obtained in 24 hours at the highest SiO_2 / Al_2O_3 ratio tested. NaA and NaP zeolites were formed under only two particular experimental conditions. The formation of these zeolites appears to be related to low alkaline concentrations and low temperatures in addition to high SiO_2 / Al_2O_3 ratios for NaP zeolite and low SiO_2 / Al_2O_3 ratios for NaA zeolite. Unlike FAU, lower reaction times may also be favorable for NaA zeolite, as was noted by Lapides and Heller-Kallai [24]. However, this study did not evaluate the possible interactions of these factors, and it is not recommended to treat them individually as influences.

Unreacted kaolinite and gibbsite reflections were observed in some samples that started from the uncalcined BT, which demonstrates the need for prior thermal treatment of the starting material to achieve the desired zeolite production [12].

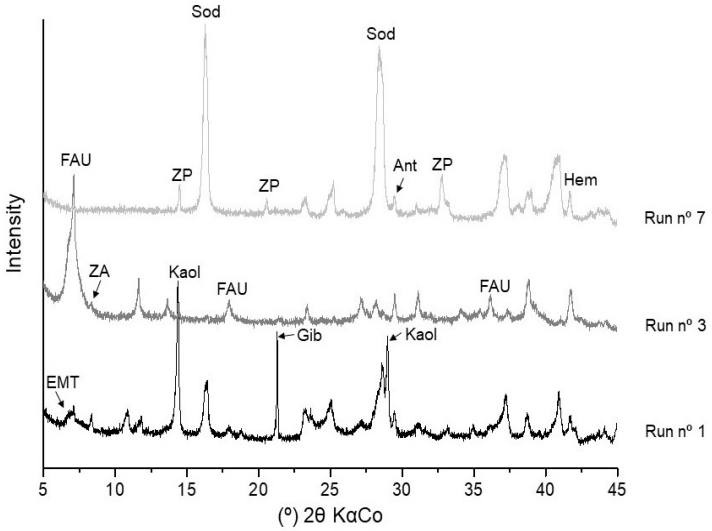

Figure 2. XRD pattern of the zeolite products obtained from the runs 1, 3 and 7 according to the experimental design. Legends: Kaol: kaolinite; Gib: gibbsite; EMT: zeolite EMT; FAU: FAU-type zeolite; ZA: zeolite NaA; ZP: zeolite NaP; Sod: basic sodalite.

Due to the predominance of sodalite in the products, the desirability tool was used to determine the experimental conditions that simultaneously favor the formation of FAU zeolite and restrict the formation of basic sodalite. Figure 3 shows the predicted values and the level curves determined by the desirability function. The results show that the temperature (variable X_3) is not statistically significant for FAU zeolite; however, it is the most influential variable to favor basic sodalite. The opposite was observed for the reaction time (X_4). Under these conditions, sodalite is favored regardless of the time; in contrast, the formation of FAU zeolite is greater at longer times.

The most determinant variable for the synthesis of zeolite material rich in FAU was observed to be the alkaline concentration of the reaction medium. This result agrees with those obtained by [14] Johnson and Arshad (2014), who observed that higher concentrations lead to decreased crystallinity of the FAU zeolite and to basic sodalite production. As in Tanaka et al. [21], Caballero et al. [12], and Gougazeh and Buhl [29], an increase of the SiO_2 / Al_2O_3 ratio was favorable for FAU, corroborating the initial expectation of the additional amorphous silica reacting with the Al_2O_3 supplied to the system by gibbsite to form the zeolite phase.

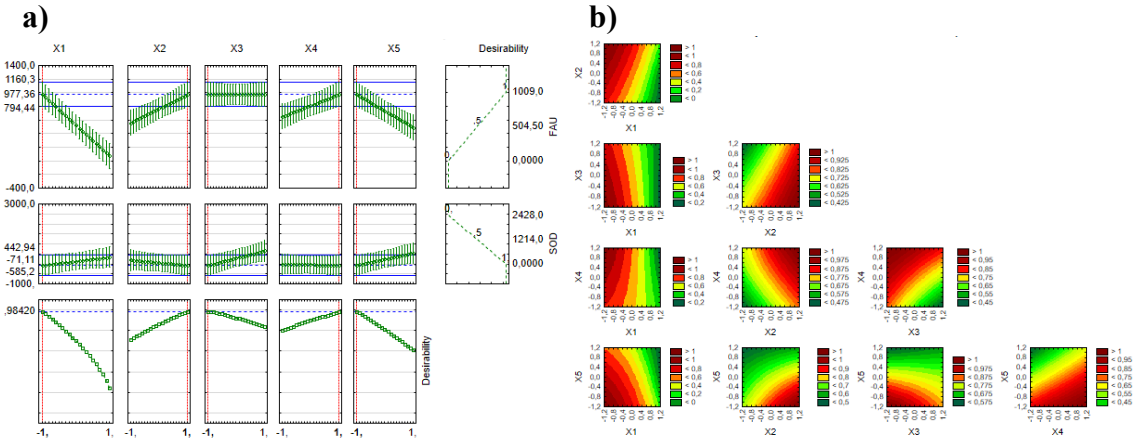

Figure 3. a) Profiles for predicted values and Desirability for FAU and basic sodalite. b) Desirability contours (method: least squares fit).

3.3. Steepest Ascent

Since the first-order model has no lack of fit, the initial experimental region showed to be far from the optimal point. Thus, the steepest ascent methodology was used to determine a new experimental region optimized to produce FAU-rich material. Based on the previous results, we established the following conditions: temperature = 70 °C and starting material = calcined. The gradient direction was then determined with the desirability function data for the most influential variable X_1 (alkaline concentration). Thereby, for each variation of $\Delta X_1 = -1$, the SiO_2 / Al_2O_3 ratio and time increased by $0.7X_2$ and $0.5X_4$ of their original values, respectively. The origin of the steepest ascent was the center point of the fractional factorial design [27].

Figure 4 shows the diffractograms of the obtained products. At the origin, sodalite is the predominant phase, and the zeolite phases FAU and EMT appear in small amounts. However, along the ascending path, the goal was satisfactorily achieved. Thus, competition between the EMT and FAU phases was initially observed, and the sodalite was continuously destroyed. Finally, under the experimental conditions of step Δ7, good crystallinity FAU zeolite is the only product.

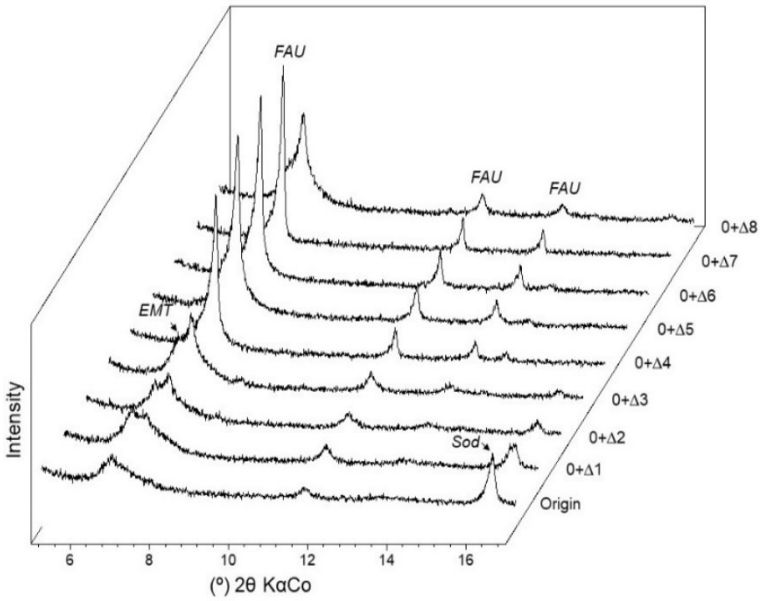

Figure 4. Comparison of the XRD patterns of the zeolite products obtained along the path of steepest ascent. Legends: EMT: zeolite EMT; FAU: FAU-type zeolite; Sod: basic sodalite.

3.4. Central Composite Design

The ANOVA data are summarized in Table 6. As observed by the p-values the linear variable X_2 (SiO_2 / Al_2O_3 ratio) and the interaction X_2X_4 (SiO_2 / Al_2O_3 ratio *x* time) are not significant. Considering the obtained regression model (equation 1), there was no detectable lack-of fit and over the studied ranges of X_1, X_2 and X_4 the fitted model was good in predicting the FAU production, despite the relative low coefficient of determination.

$$FAU_{(d_{111})\text{intensity}} = 1735{,}50 - 260{,}35X_1 - 191{,}99X_1^2 + 34{,}52X_2 + 224{,}15X_2^2 + 79{,}22X_4 + 134{,}86X_4^2 + 145{,}62X_1X_2 + 80{,}12X_1X_4 - 48{,}37X_2X_4 \quad (R^2 = 0{,}7677) \qquad (1)$$

Table 6. ANOVA for the 2^3 Central Composite Design.

Variables	SS	df	MS	F	p-value
X_1	924882	1	924882.0	4624.410	0.009361
X_1^2	340640	1	340640.4	1703.202	0.015423
X_2	16258	1	16258.3	81.291	0.070321
X_2^2	464320	1	464319.5	2321.598	0.013211
X_4	85629	1	85628.8	428.144	0.030743
X_4^2	168084	1	168084.2	840.421	0.021951
X_1X_2	169653	1	169653.1	848.266	0.021850
X_1X_4	51360	1	51360.1	256.801	0.039675
X_2X_4	18721	1	18721.1	93.606	0.065568
Lack of Fit	859683	5	171936.5	859.683	0.025888
Pure Error	200	1	200.0		
Total	3702401	15			

Figure 5 shows the response surfaces for the alkaline concentration, SiO_2 / Al_2O_3 ratio and reaction time (variables X_1, X_2, and X_4, respectively) in the optimized region. The obtained model reveals a saddle-like surface. In this type of model, it is more difficult to find a critical point because there is more than one maximum point, and the true optimum can be "lost in the shuffle" [30]. Despite this, good results for crystalline FAU synthesis can be obtained establishing an alkaline concentration of 126 g/L (variable X_1 with a fixed level = 0.7) and lower values of the SiO_2 / Al_2O_3 ratio and time (SiO_2 / Al_2O_3 = 1.82 and time = 74 h), as observed on the response surfaces.

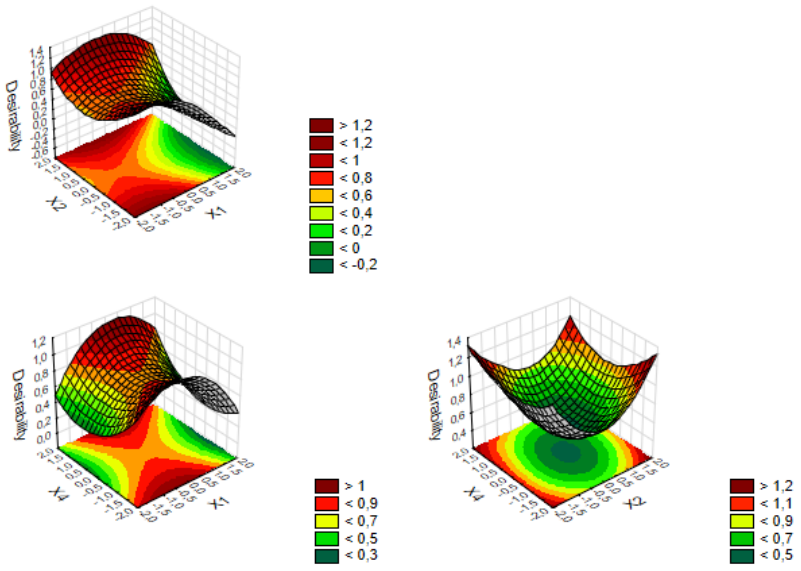

Figure 5. Desirability response surface/contours of the FAU-type zeolite as function of the variables (Coded Variables values) X_1 = alkaline concentration; X_2 = SiO_2 / Al_2O_3 molar ratio and; X_4 = time.

The diffractograms (Figure 6) show that the alkaline concentration is the determinant variable of the process. Over a narrow range tested, it was observed that at higher concentrations (above 140 g/L), there is a decrease of crystallinity and competition between the FAU and EMT phases. At lower concentrations, FAU is the only phase that formed, with well-resolved diffraction peaks.

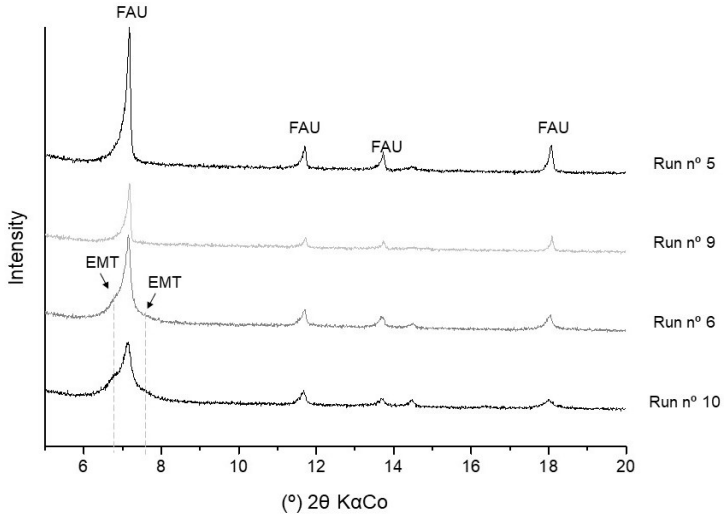

Figure 6. Comparison of the zeolite products highlighting the influence of alkaline concentration (runs n° 5 and 9 at lower level and n° 6 and 10 at higher levels). Legends: EMT: zeolite EMT; FAU: FAU-type zeolite.

The Figure 7 shows the SEM micrographs of the raw material (BT) and the zeolitic product (run nº 5). The fine-grained raw material is observed as small irregular aggregates (~5 µm), while in the product is observed large aggregate composed by small grains of FAU zeolite. It was not found large crystals domains with FAU characteristic shape (octahedral) as reported by Moneim and Ahmed [31] and Garcia et al. [32] showing that the degree of crystallinity is not so high for this FAU zeolite. This is probably due the syntheses were made from a waste where some impurity may influence [23] and no aging was taken [33]. In addition, there could be some amorphous Al_2O_3 from gibbsite unreacted and the FAU zeolite nucleation/crystallization appears to take place on the surface of unreacted gibbsite. However, the EDS results shown corroborate with the XRD results that the aggregates are mainly FAU zeolite and amorphous material are apparently non-existent.

The nitrogen adsorption isotherms of the raw material (BT) and zeolitic product (run nº 5) are present in the Figure 8. The raw material presents an isotherm type II while the zeolitic product shows an isotherm type IV. It is observed a specific surface area and pore volume in good agreement with those reported for FAU zeolites [34, 35]. In comparison with the raw material (BT) the specific surface area raised from 58.26 m^2g^{-1} to 324.11 m^2g^{-1}.

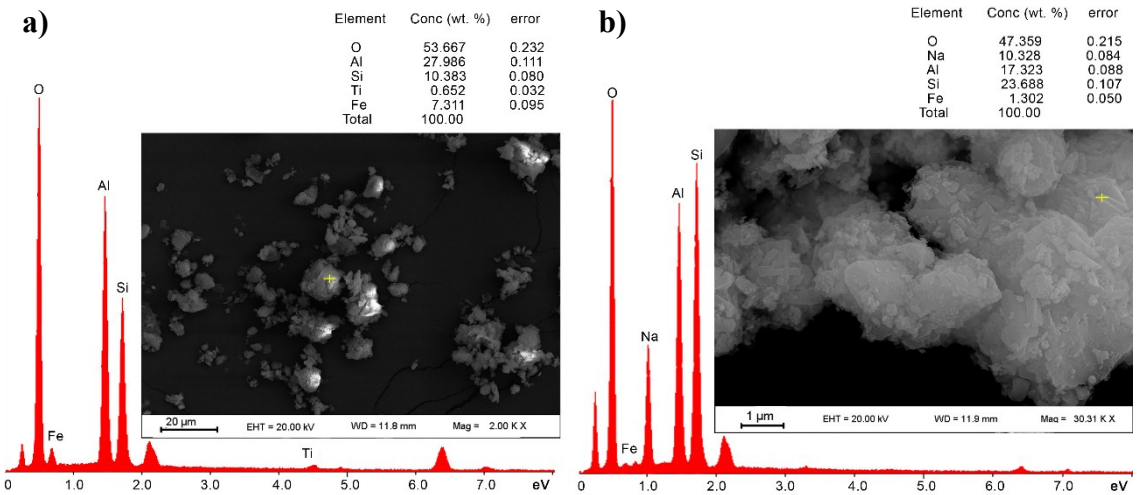

Figure 7. SEM/EDS images. a) raw material (BT). b) zeolite product (run n° 5).

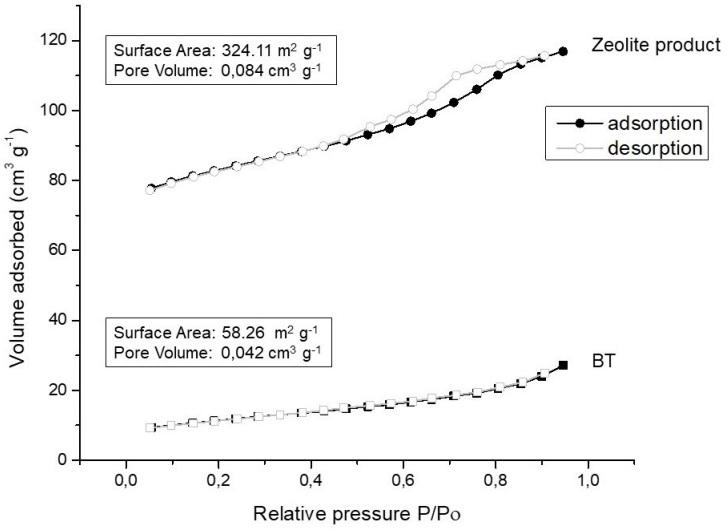

Figure 8. N_2 adsorption-desorption isotherms. a) raw material (BT); b) zeolite product (run n° 5).

4. Conclusion

The objective to produce FAU zeolite from the Mineração Paragominas SA bauxite tailings was successfully achieved. This approach can represent an economical proposal and environmentally friendly, using this abundant waste as a cheap material to produce zeolites. Of course, it is extremely necessary not only evaluate the technical feasibility, but also the performance, application, costs and marked demand for this product. This assessment is ongoing.

To produce FAU zeolite, the synthesis parameters were optimized using a sequential factorial design methodology. The results showed that the most influential factors in the hydrothermal synthesis process are the alkalinity, SiO_2 / Al_2O_3 ratio and time. Calcination of the Bauxite Tailings is needed in order to favor the FAU zeolite and avoid the formation of basic sodalite. In addition, higher temperatures strongly favor the formation of sodalite.

The regression model showed a satisfactory fit. The response surface had a saddle profile which indicates that there is more than one optimal condition for FAU zeolite synthesis. In this context, considering a low consumption of the raw material and time, the best condition proposed to produce FAU zeolite from the Bauxite Tailings are: alkaline concentration = 126 g/L, SiO_2 / Al_2O_3 ratio = 1.82, time = 74 h, temperature = 70 ºC and calcined material.

5. References

1. Brasil. SUMÁRIO MINERAL Departamento Nacional de Produção Mineral. Sumário Mineral/Coordenadores Thiers Muniz Lima, Carlos Augusto Ramos Neves Brasília: DNPM, 2018. 131 p.
2. A.A.B. Maia, E. Saldanha, R.S. Angélica, C.A.G. Souza, R.F. Neves. Utilização de rejeito de caulim da Amazônia na síntese da zeólita A. *Cerâmica*, Vol. 53, (2007), 319–324.
3. R.A. Menezes et al., Synthesis of ultramarine pigments from Na-A zeolite derived from kaolin waste from the Amazon. *Clay Miner*. Vol. 52, (2017), 83–95.
4. A.A.B. Maia, Angélica, R.F. Neves. Estabilidade térmica da zeólita A sintetizada a partir de um rejeito de caulim da Amazônia. *Cerâmica*, Vol. 54, (2008), 345–350.
5. S.P.A. Paz, R.S. Angélica, R.F. Neves. Síntese hidrotermal de sodalita básica a partir de um rejeito de caulim termicamente ativado. *Quim. Nova*, Vol. 33, (2010), 579–583.

6. L.G. Nascimento, S.P.A. Paz, R.S. Angélica, H. Kahn. Síntese de Zeólitas a Partir Do Rejeito Gibbsítico/Caulinítico Do Beneficiamento de Bauxita de Paragominas-PA. *57º Congresso Brasileiro de Cerâmica 5º Congresso Iberoamericano de Cerâmica,* (2013), 1019–1029.
7. E.A. Hildebrando, R.S. Angélica, R.F. Neves, F.R. Valenzuela-Diaz. Síntese de zeólita do tipo faujasita a partir de um rejeito de caulim. *Cerâmica*, Vol. 58, (2012), 453–458.
8. E.A. Hildebrando et al., Synthesis and characterization of zeolite NaP using kaolin waste as a source of silicon and aluminum. *Mater. Res.* Vol. 17, (2014), 174–179.
9. R.A. Menezes et al., Color and shade parameters of ultramarine zeolitic pigments synthesized from kaolin waste. *Mater. Res.* Vol. 17, (2014), 23–27.
10. A.S. Kovo. Effect of temperature on the synthesis of zeolite X from ahoko nigerian kaolin using novel metakaolinization technique. *Chem. Eng. Commun.* Vol. 199, (2012), 786–797.
11. C.H. Rüscher et al., Relation between growth-size and chemical composition of X and Y type zeolites. *Microporous Mesoporous Mater.* Vol. 92, (2006), 309–311.
12. I. Caballero, F.G. Colina, J. Costa. Synthesis of X-type zeolite from dealuminated kaolin by reaction with sulfuric acid at high temperature. *Ind. Eng. Chem. Res.* Vol. 46, (2007), 1029–1038.
13. H. Lechert. The pH value and its importance for the crystallization of zeolites. *Microporous Mesoporous Mater.* Vol. 22, (1998), 519–523.
14. E.B.G. Johnson, S.E. Arshad. Hydrothermally synthesized zeolites based on kaolinite: A review. *Appl. Clay Sci.* Vol. 97–98, (2014), 215–221.
15. T. Abdullahi, Z. Harun, M.H.D. Othman. A review on sustainable synthesis of zeolite from kaolinite resources via hydrothermal process. *Adv. Powder Technol.* Vol. 28, (2017), 1827–1840.
16. A.E. Ameh et al., Influence of aluminium source on the crystal structure and framework coordination of Al and Si in fly ash-based zeolite NaA. *Powder Technol.* Vol. 306, (2017), 17–25.
17. J. Rocha, J. Klinowski, J.M. Adams. Synthesis of zeolite Na-A from metakaolinite revisited. *J. Chem. Soc., Faraday Trans.* Vol. 87, (1991), 3091–3097.
18. A. Gualtieri et al., Kinetics of formation of zeolite NaA [LTA] from natural kaolinites. *Phys. Chem. Miner.* Vol. 24, (1997), 191–199.
19. A.A.B. Maia et al., Use of 29Si and 27Al MAS NMR to study thermal activation of kaolinites from Brazilian Amazon kaolin wastes. *Appl. Clay Sci.* Vol. 87, (2014), 189–196.
20. M. Noack et al., Molecular sieve membranes for industrial application: Problems, progress, solutions. *Chem. Eng. Technol.* Vol. 25, (2002), 221–230.
21. H. Tanaka, S. Furusawa, R. Hino. Synthesis, characterization, and formation process of Na-X zeolite from coal fly ash. *J. Mater. Synth. Process.* Vol. 10, (2002), 143–148.
22. A.S. Kovo, S.M. Holmes. Effect of aging on the synthesis of kaolin-based zeolite Y from Ahoko Nigeria using a novel metakaolinization technique. *J. Dispers. Sci. Technol.* Vol. 31, (2010), 442–448.
23. M. Murat et al., Synthesis of Zeolites from Thermally Activated Kaolinite. Some Observations on Nucleation and Growth. *Clay Miner.* Vol. 27, (1992), 119–130.
24. I. Lapides, L. Heller-Kallai. Reactions of metakaolinite with NaOH and colloidal silica - Comparison of different samples (part 2). *Appl. Clay Sci.* Vol. 35, (2007), 94–98.
25. L. Heller-Kallai, I. Lapides. Reactions of kaolinites and metakaolinites with NaOH-comparison of different samples (Part 1). *Appl. Clay Sci.* Vol. 35, (2007), 99–107.
26. H. Youssef, D. Ibrahim, S. Komarneni. Microwave-assisted versus conventional synthesis of zeolite A from metakaolinite, *Microporous Mesoporous Mater.* Vol. 115, (2008), 527–534.
27. G.E.P. Box, J.S. Hunter, W.G. Hunter. Statistics for Experimenters: Design, Innovation, and Discovery, 2nd ed. Wiley, New York (2005).

28. D.C. Montgomery. Design and Analysis of Experiments, 8th ed. John Wiley & Sons, Inc., USA (2012).
29. M. Gougazeh, J.-C. Buhl. Synthesis and characterization of zeolite A by hydrothermal transformation of natural Jordanian kaolin. *J. Assoc. Arab Univ. Basic Appl. Sci.* Vol. 15, (2014), 35–42.
30. M.J. Anderson, P.J. Whitcomb. DOE Simplified: Practical Tools for Effective Experimentation. 3rd ed. CRC Press (2016).
31. M.A. Moneim, E.A. Ahmed. Synthesis of Faujasite from Egyptian Clays: Characterizations and Removal of Heavy Metals. *Geomaterials*, Vol. 5, (2015), 68-76.
32. G. Garcia, et al., Selective synthesis of FAU-type zeolites. *J. Cryst. Growth*, Vol.489, (2018), 36–41.
33. H. Jülide Köroğlu et al., Effects of low-temperature gel aging on the synthesis of zeolite Y at different alkalinities. *J. Cryst. Growth*, Vol. 241 (4), (2002), 481–488.
34. U. Lohse et al., Cubic and hexagonal faujasites with varying Si/Al ratios I. Synthesis and characterization. *Appl. Catal., A,* Vol.129, (1995), 189–202.
35. Y. Ma et al., Synthesis and characterization of 13X zeolite from low-grade natural kaolin. *Adv. Powder Technol.* Vol. 25, (2014), 495–499.